Heliyon 9 (2023) e18788

Contents lists available at ScienceDirect

Heliyon

journal homepage: www.cell.com/heliyon

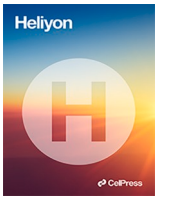

Facile fabrication of Nishamalaki churna mediated silver nanoparticles with antibacterial application

Bhavna Ghosh [a,b], Anindya Bose [a,*], Ankita Parmanik [a], Sanjay Ch [c], Milan Paul [c], Swati Biswas [c], Goutam Rath [a], Debapriya Bhattacharya [d]

[a] School of Pharmaceutical Sciences, Siksha O Anusandhan (Deemed to Be University), Bhubaneswar, Odisha, 751003, India
[b] Sri Jayadev College of Pharmaceutical Sciences, Naharkanta, Via: Balianta, Bhubaneswar, Odisha, 752101, India
[c] Department of Pharmacy, Birla Institute of Technology & Science-Pilani, Hyderabad Campus. Jawahar Nagar, Kapra Mandal. Medchal District, Telangana, 500 078, India
[d] Center for Biotechnology, Siksha O Anusandhan (Deemed to Be University), Bhubaneswar, Odisha, 751003, India

ARTICLE INFO

Keywords:
Antimicrobial resistance
Biofilm
Green synthesis
Ayurvedic formulation
Amlaki
Turmeric

ABSTRACT

Antimicrobial resistance (AMR) is one of the most serious threats to today's healthcare system. The prime factor behind increasing AMR is the formation of complex bacterial biofilms which acts as the protective shield between the bacterial cell and the antimicrobial drugs. Among various nanoformulations, green synthesized metallic silver nanoparticles are currently gaining research focus in safely breaking bacterial biofilms due to the inherent antimicrobial property of silver. In the current work, the aqueous extract of the ayurvedic formulation Nishamalaki churna is used to exhibit one pot green synthesis of silver nanoparticles. The physicochemical characteristics of Nishamalaki churna extract mediated AgNPs were evaluated using various analytical techniques, like UV–Visible spectrophotometer, FT-IR spectroscopy, SEM, XRD, DLS-Zeta potential analyzer etc. The synthesized spherical AgNPs were well formed within the size range of 30 nm to 80 nm. Furthermore, the synthesized AgNPs showed potent antibacterial effects against two primary AMR-causing bacterial species like *Staphylococcus aureus* and *Pseudomonas aeruginosa* with the successful destruction of their biofilm formation. Additionally, these AgNPs have shown profound antioxidant and anti-inflammatory activities as desirable add-on effects required by a prospective antibacterial agent.

1. Introduction

Antimicrobial resistance (AMR) is regarded as one of the major health threats in modern times. In the year 2019, an estimated 4.95 million deaths were worldwide reported by various illnesses with as many as 1.27 million deaths by AMR alone. This figure was much higher than the number of people who died due to AIDS or malaria in that year [1]. The continuous reduction in the effective antibiotic options against microbes is the major cause behind this AMR. Furthermore, microbial biofilm formation strengthens resistant microbes by obstructing penetration of antimicrobial agents into them. Biofilms are now responsible for up to 60% of all human infections [2]. In comparison to logarithmic-phase planktonic cells, biofilms are extremely resistant to bactericidal antimicrobials. This antibiotic scarcity against resistant bacteria has created an urgency and highly augmented pressure to invent new therapeutics and strategies to

* Corresponding author.
E-mail address: anindyabose_in@yahoo.com (A. Bose).

https://doi.org/10.1016/j.heliyon.2023.e18788
Received 11 April 2023; Received in revised form 27 July 2023; Accepted 27 July 2023
Available online 28 July 2023

break the shackles of AMR by antibiofilm activity.

Silver has been used as a medicinal agent for many years due to its inherent antimicrobial property [3]. Currently, silver nanoparticles (AgNPs) have received considerable attention as potential antimicrobial agents. However, their synthesis using environmentally hazardous chemicals add to the inherent toxicity of silver ions and makes them unsafe for therapeutic applications [4]. This fact has prompted the popularity of environment-friendly alternatives and less toxic 'green' synthesis roots of AgNPs utilizing plant and plant products, bacteria, fungi, algae, yeast, and viruses. In this regard, plants contain a variety of phytoconstituents that can serve dual purposes by acting as natural reducing/capping agents in the AgNPs synthesis as well as shrinking the inherent toxicity of silver [5].

Nishamalaki Churna is an Ayurvedic powder formulation containing an equi-proportional mixture of two herbal ingredients, namely Amlaki (*Emblica officinalis*) fruits and Turmeric (*Curcuma longa*) rhizome [6]. Major phytoconstituents of Amlaki such as gallic acid, trans cinnamic acid, methyl gallate, quercetin-3-O-α-arabinofuranoside, emblifatmin etc. possess remarkable antioxidant properties, which are expected to act as a reducing agent for reducing the silver salt in the green synthesis of AgNPs [7]. The phytochemicals present in Amlaki, are also responsible for its potent antibacterial activity. Turmeric also possesses several therapeutic activities [8,9] like antimicrobial, anti-inflammatory, anticancer, antitumor, antioxidant activities etc. Curcumin, the principal active component of turmeric, is mostly responsible for the observed bioactivities of this herb. The AgNPs synthesis with both these two individual plants and their biological activity evaluation have been already reported [8–13], however, there is no report about the green synthesis of AgNPs from Nishamalaki Churna and assessment of its antimicrobial activities. In Ayurvedic system of medicine, Nishamalaki churna itself is marketed and prescribed as a drug as such. However, Nishamalaki churna administration to the patients may be proven ineffective due to the poor bioavailability of its active phytoconstituents from the powdered mixture of its herbal ingredients as well as it may be inconvenient to administer in such patients. This encouraged us to develop Nishamalaki churna mediated metal nanoparticle formulations and evaluate its antibacterial effect.

The experimental data on the biosynthesis of metal nanoparticles using polyherbal formulation are limited in number and need to be explored. In this regard, two recent reports have described the sustainable and environmentally friendly production of iron oxide and silver nanoparticles from Triphala churna extract, another well-known traditional remedy [14,15]. In the current study, we have made a contribution to the creation of novel antimicrobials to combat against antimicrobial resistance (AMR) by synthesizing silver nanoparticles from the aqueous extract of Nishamalaki Churna and assessing their antibacterial and antibiofilm properties against both gram-positive and gram-negative pathogens.

2. Materials and methods

2.1. Materials

Silver nitrate was purchased from Nice Chemicals (P) Ltd., Kerala, India. The components of Nishamalaki i.e., dried fruits of Amla (*Emblica officinalis*) and dried rhizome of Turmeric (*Curcuma longa*) were purchased from local herbal shop followed by its authentication by a local botanist. Doubled distilled water was utilized throughout the experimental procedure.

2.2. Preparation of Nishamalaki churna extract

The Nishamalaki churna was prepared by mixing equal parts of dry powder of Amla and Turmeric. To develop the churna, the two plant components were individually ground into a fine powder, put through sieve number 60, and blended in an exact ratio. In the next step, 10 mg of churna was mixed with 10 mL of double-distilled water. After being heated for 20 min at 60 °C, the mixture was filtered before being cooled. The fresh polyherbal extract simultaneously served as both reducing and capping agent in the formation of AgNPs.

2.3. Synthesis of Nishamalaki mediated silver nanoparticles

The AgNPs were synthesized by heating 95 mL of 1 mM silver nitrate with 5 mL of Nishamalaki Churna extract at 80 °C with constant stirring for 1 h. The gradual colour change of the mixture solution from yellowish orange to brownish grey indicated the completion of the synthesis, which was further confirmed by UV–visible spectroscopical investigation (JASCO V-630). On completion of the reaction, the mixture underwent a centrifugation at 12,000 rpm for 20 min, followed by washing with double distilled water, to remove the impurities.

The experimental conditions like concentration of the silver salt solution and plant extract, heating and stirring conditions, pH and reaction time were optimized by trial-and-error.

2.4. Characterization techniques

The extracts of Nishamalaki Churna and its two ingredients were subjected to HPTLC fingerprinting analysis by an HPTLC instrument (CAMAG) [16]. These three solutions were individually spotted at two different concentrations (2 μL and 5 μL) by the Linomat 5 auto sample applicator on a commercially available Silica gel 60 F_{254} HPTLC plate (10 cm × 10 cm). The sports were allowed to develop by mobile phase of toluene: ethyl acetate: methanol: formic acid (3:3:3:1) in the twin trough development chamber. After drying, the retention factor (R_f) values of the developed spots were documented using winCAT software after visualization at specific wavelengths (254 nm, 366 nm and 540 nm). The aqueous Nishamalaki churna extract was subjected to qualitative testing for the presence of major phytoconstituents by standard methods [17]. Additionally, quantitative determination of total phenolics and

total flavonoids was performed using Gallic acid and Quercetin as standard respectively [18,19].

The morphological structure of the AgNPs was determined by a Scanning Electron Microscope (NOVA NANOSEM 450) by evenly dispersing them as a thin layer on an adhesive carbon tape fastened to aluminium stubs. After the stubs had been coated with gold of the correct thickness, AgNPs were analyzed at 20 kV [20]. The zeta potential of synthesized AgNPs was analyzed by dynamic light scattering through Zetasizer 3600 (Malvern Instruments Ltd.). The sample's particle size and the polydispersity index (PDI) values were also assessed before and after carrying out the lyophilization of the sample by freeze-drying method. Briefly, the NPs solution and cryoprotectant-like mannitol at a concentration of 5% w/v were used and kept at −80 °C for 6 h. The frozen product was kept for lyophilization at −99 °C until the free-flowing powder is obtained. The particle size was measured using a Malvern Zetasizer 3600 (Malvern Instruments Ltd) equipped with a 10-mW He–Ne laser (633 nm) and operating at an angle of 90° and a temperature of 20 °C. The samples of AgNPs were diluted 1:20 with a 0.9% (w/w) solution of NaCl in distilled water to eliminate the primary charge effect. A sample volume of 2 mL was used in 10 mm diameter cuvettes (Sarstedt, Germany).

The Nishamalaki mediated AgNPs were subjected to FT-IR analysis (JASCO FT/IR-4600) using the ATR technique. The scanning range was kept from 4000 cm^{-1} to 400 cm^{-1} [21] and the spectra were interpreted for further detailing. To study the crystallinity of synthesized AgNPs, dried powdered form of green synthesized silver nanoparticles was subjected to X-RD analysis (Rigaku Ultima IV) at 2Θ range of 10°–70° at a rate of 10°/min using a voltage of 40 kV, 30 mA.

2.5. Evaluation of biological activities

2.5.1. Antimicrobial and antibiofilm action

The antibacterial and antibiofilm properties of the produced AgNPs were assessed for both gram-positive (*Staphylococcus aureus*) and gram-negative bacteria (*Pseudomonas aeruginosa*). The bacterial strains were cultured aerobically for the entire night at 37 °C and 85% relative humidity in Luria Bertani (LB) Broth, Miller. The next day a subculture was incubated at 37 °C (200 μL of overnight culture in 5 mL of LB broth) for 2hrs to get an OD_{600} of 0.2 for *P. aeruginosa* and 0.6 for *S. aureus.* All the bacteria were pelleted and resuspended in 1 mL LB broth; serial diluted with PBS (pH 7.4) before determination of the antimicrobial activity.

2.5.1.1. Minimum inhibitory concentration (MIC) and minimum bactericidal concentration (MBC) determination. These experiments were conducted using a modified version of the microtiter broth dilution technique. Briefly, bacteria were diluted to 10^6 CFU/mL in LB broth, and 100 μL of the bacterial culture was incubated at 37 °C with 100 μL AgNPs of various concentrations (0–64 μg/mL) in a 96 well plate. MIC/MBC was determined at different time points by observing visible turbidity as well as the measurement of the optical density of the cultured broths at 600 nm. The data was presented as the mean of three replications [Fig. 7 (a)].

2.5.1.2. Zone of inhibition study. The zone of inhibitions for the above cultured micro-organisms was determined after treatment with synthesized AgNPs at 8, 16 and 32 μg/mL concentrations. The sterile spreaders were used to spread the lawn of bacteria on nutrient agar plates. The AgNPs soaked in sterile circular paper discs were put on the bacterial lawn and incubated for 24 h. The growth inhibition zones were measured after the incubation, and the pictures were captured using a digital camera.

2.5.1.3. Live/dead assay on biofilms. P. aeruginosa and *S. aureus* (10^6 CFU/mL) in LB Broth (Miller) were incubated on coverslips in a 12-well plate at 37 °C, and 85% relative humidity for 2 days. The next day coverslips were removed and washed with Phosphate-buffered saline (PBS) for further studies. Planktonic bacterial films (10^6 CFU, 1 mL) of both *P. aeruginosa* and *S. aureus* were incubated with various concentrations of AgNPs containing 8,16 and 32 μg/mL for 4 h at 37 °C (under shaking). Two washes with sterile physiological saline solution (0.9% w/v NaCl) were performed on the bacterial films. The obtained film was stained using SYTO 9 and Propidium iodide (PI) fluorescent stains. The staining solution was prepared by mixing SYTO 9 and PI at concentrations 33.4 μM and 0.4 mM, respectively. The bacteria staining was performed by adding 3 μL and 5 μL of SYTO 9: PI (1:1) for *P. aeruginosa* and *S. aureus*, respectively, and kept in the dark for 10min. After the staining, the bacteria's images were captured by stacking to a penetration depth of 20 μM using a confocal fluorescence microscope (Leica, DMi8, Germany) followed by a 3D image generation for analysis.

2.5.2. Antioxidant activity and anti-inflammatory activity

The antioxidant property of synthesized AgNPs was measured in terms of the percentage inhibition of DPPH (2,2-diphenyl-1-picryl-hydrazyl-hydrate) free radicals at 520 nm using Ascorbic acid as a standard drug [22–24]. To assess their anti-inflammatory effect, the percentage inhibition of protein denaturation was assessed [24,25]. Briefly, 1 mL of sample solution was mixed with 5 mL of 1% solution of Bovine serum albumin following the pH adjustment to 6.3 with 1 N HCl. The absorbance was measured at 660 nm after an incubation period of 30 min.

2.5.3. Cell viability study

The viability of cell on treatment with synthesized AgNPs was studied by MTT assay using Human embryonic kidney (HEK 293) cell lines. In this method, 100 μL of the cell suspension was added into 96 well plates each well with a concentration of 10,000 cells per well. The plates were incubated after treatment with AgNPs for 24 h–48 h. After the end of treatment period, 50 μL of MTT reagent at a concentration of 5 mg/mL was added into each well and again incubated for 4 h before adding 150 μL DMSO to dissolve the formed

purple formazan crystals. After 1 h, the absorbance was measured at 570 nm and 620 nm using Spectramax Multiplate reader (Molecular Devices, USA).

3. Results and discussions

The present work focuses on the investigation of the antibacterial efficacy of green synthesized silver nanoparticles (AgNPs) obtained by the aqueous extract of Nishamalaki Churna. It is an already proven fact that AgNPs have outstanding possibilities as antibacterial agents [26–29]. On the other hand, Nishamalaki Churna possesses potent bioactivities like antibacterial, anticancer, antitumor, anti-inflammatory, and antioxidant activities. The Nishamalaki Churna mediated green synthesized AgNPs, therefore, have been evaluated as a prospective antibacterial agent.

3.1. HPTLC fingerprinting of Nishamalaki churna extract

The R_f values obtained in the chromatogram under different visualizing conditions such as UV light [Fig. 1(A)], Fluorescence light [Fig. 1(B)] and Visible light [Fig. 1 (C)] revealed the presence of major phytoconstituents in the extract. The R_f values of 0.77 and 0.82 in the Nishamalaki extract respectively indicated the presence of Amlaki and turmeric in the formulation.

3.2. Phytochemical analysis of herbal extract

It was noticed that the Nishamalaki churna extract holds a satisfactorily balanced phytochemical pattern for the synthesis and stabilization of AgNPs. Among these phytoconstituents, carbohydrates can control the spherical shape and size of the AgNPs, phenols and flavonoids help in faster as well as a greater amount of AgNPs synthesis and polysaccharides are associated with both capping and reducing activity [3]. The quantitative assay for phenolic content and flavonoid content (Table 1) reveals that the aqueous extraction of Nishamalaki Churna contains high amount of flavonoids and phenols. These phytoconstituents can serve as a potent reducing agent to felicitate the faster synthesis of AgNPs as well as an aid towards the antioxidant property of synthesized nanoparticles [11,30,31].

3.3. Bio-synthesis of silver nanoparticles

The Nishamalaki churna extract aided green synthesized AgNPs were best formed within one and half hour at 80 °C with constant stirring. The process involved for synthesizing the nanoparticles is presented in Fig. 2. During the course of reaction, aliquots of reaction mixture were analyzed through UV–Visible spectrophotometer to check the formation of silver nanoparticles along with observing the gradual colour change. The completion of the reaction was marked by the colour change from yellow to dark brown with the occurrence of UV–Visible absorption maxima at 442 nm [20,32]. A confirmation of the product formation is shown by plotting the spectral overlay pattern of Nishamalaki extract, silver salt solution and their reaction mixture with the formation of AgNPs [Fig. 3].

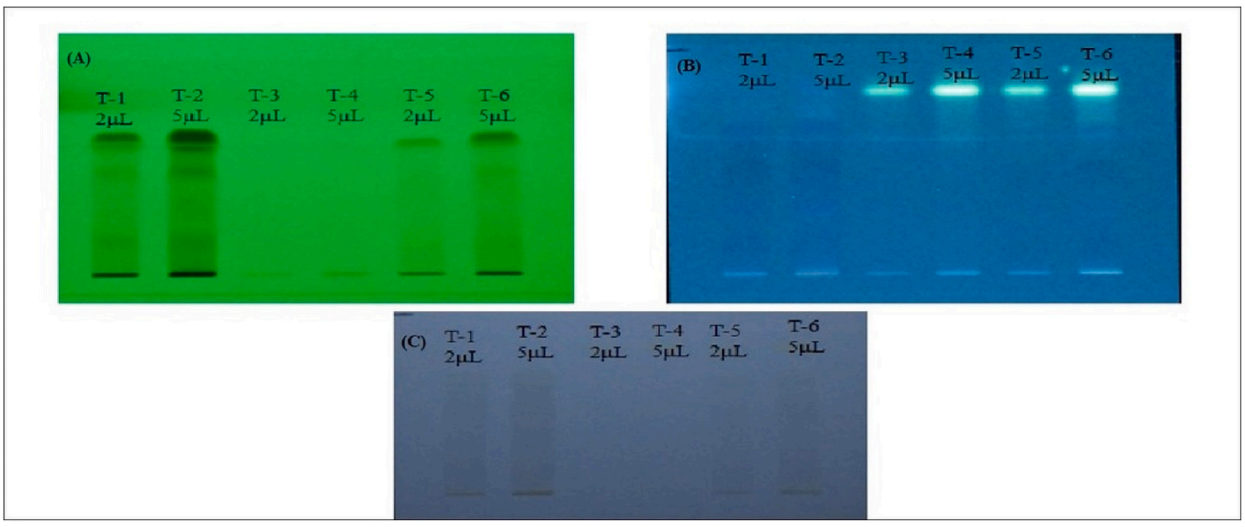

Fig. 1. HPTLC image of aqueous amla extracts (T-1 and T-2), aqueous turmeric extracts (T-3 and T-4) and aqueous Nishamalaki churna extracts (T-5 and T-6), each applied at two different volumes (2 μL and 5 μL), under (A) 254 nm, (B) 366 nm, (C) 540 nm.

Table 1
Assay of total phenol and flavonoid content of Nishamalaki Churna aqueous extract.

Assay	Nishamalaki Churna extract
Total phenolic content (mg of GAE/g)	24.46 ± 0.02
Total flavonoid content (mg of QE/g)	71.62 ± 0.03

Values are expressed as Mean ± S.D (n = 3).

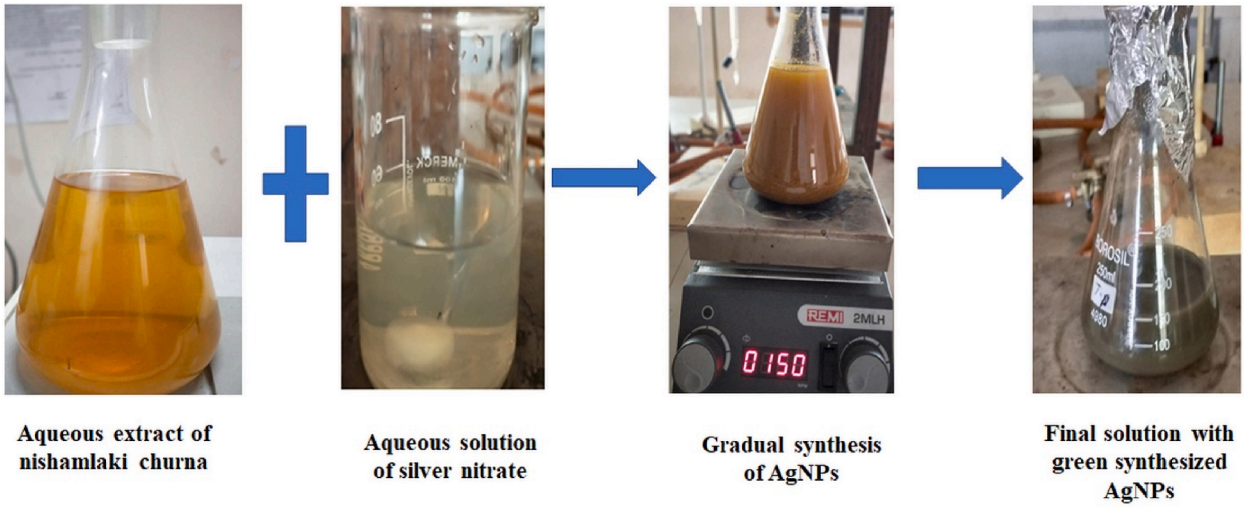

Fig. 2. The process of silver nanoparticles green synthesis by the aqueous Nishamalaki Churna extract. (For interpretation of the references to colour in this figure legend, the reader is referred to the Web version of this article.)

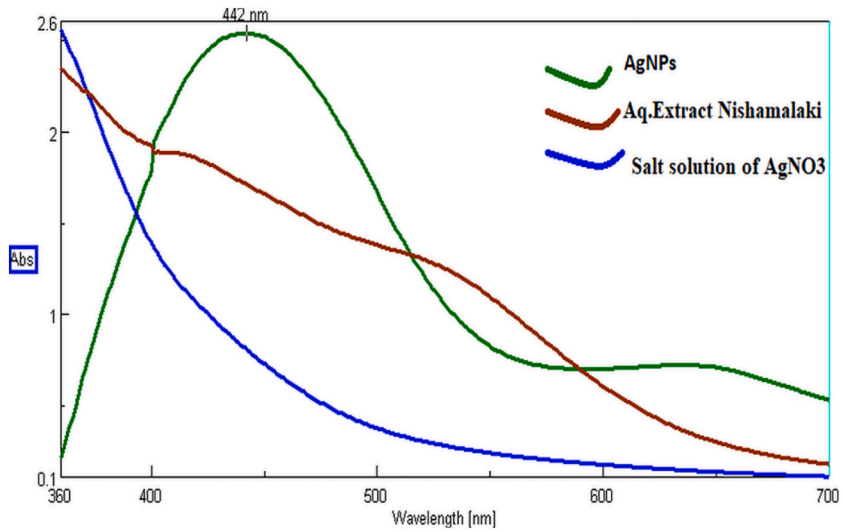

Fig. 3. UV–Visible spectrophotometric study on synthesis of Nishamalaki churna mediated silver nanoparticles.

3.4. Characterization of green synthesized silver nanoparticles

3.4.1. Scanning electron microscopy

SEM analysis of green synthesized silver nanoparticles was done to get an idea about the surface morphology of nanoparticles. According to SEM images [Fig. 4], the generated silver nanoparticles were within 48–90 nm size range. The appearance of clusters could be due to the agglomeration tendency of the synthesized AgNPs.

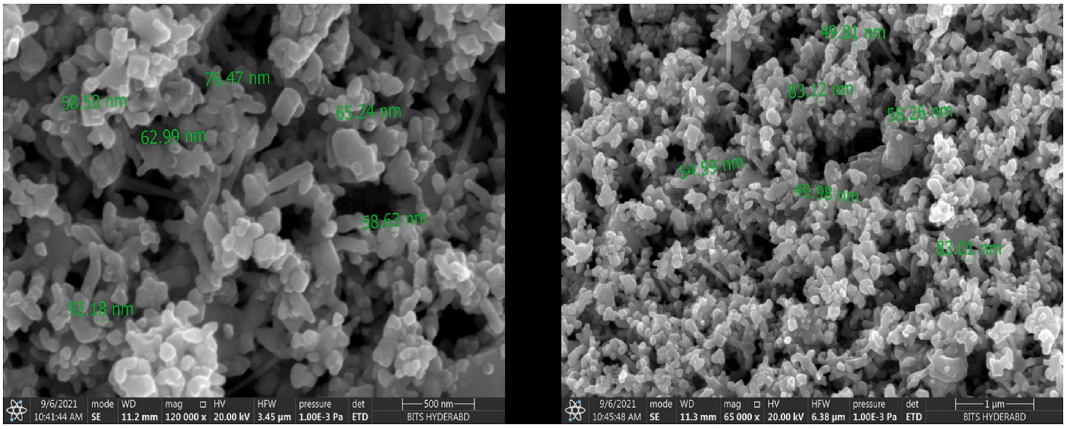

Fig. 4. SEM images of synthesized AgNPs.

3.4.2. Dynamic light scattering (DLS) and zeta potential

The average size distribution of AgNP particles was found to be 107 ± 3.56nmat PDI of 0.238 ± 0.02, which revealed that they were of good quality [Fig. 5]. The greater size compared to the SEM results might have indicated their tendency to agglomerate on long-standing [33,34].

The electrical charge of attraction or repulsion between the nanoparticles in their colloidal suspension is measured by the zeta potential. The synthesized AgNPs had a positive zeta potential of 1.22 ± 0.56. The surfaces of the nanoparticles were positively charged due to the presence of positive functional groups like protonated amines.

3.4.3. FTIR analysis

The synthesized silver nanoparticles contain a variety of functional groups [Fig. 6(a)] that ensures the existence of phytochemicals responsible for synthesis, stabilization and capping of silver nanoparticles. The peak at 3198 cm^{-1} is indicative of the presence of Aromatic C=H stretching. The stretching vibration of the aliphatic -C-H group and the carbonyl group (C=O) is responsible for the peaks found at 2922 cm^{-1} and 1643 cm^{-1}, respectively. The presence of -C-O-C (ester group) is indicated by the peak at 1025 cm^{-1}.

3.4.4. XRD analysis

Analyzing the X-ray powder diffraction can help identify a product's crystalline makeup. The intensity and position of peaks confirm the crystalline nature of silver nanoparticles [25,35]. Major peaks at 38.2° (111), 44.4° (200), 64.6° (220) and 77.4° (311) indicated the typical face-centered cubic structure of green synthesized silver nanoparticles [Fig. 6(b)]. The average crystallite size of formulated AgNPs, calculated by the Debye-Scherrer equation, was found to be 24.42 nm. Apart from the major peaks of silver nanoparticles, some other peaks were seen to be present at 27.9°, 32.3°, 55.4°, 67.6° which can be considered as the peaks of biogenic materials present in the extract of Nishamalaki churna.

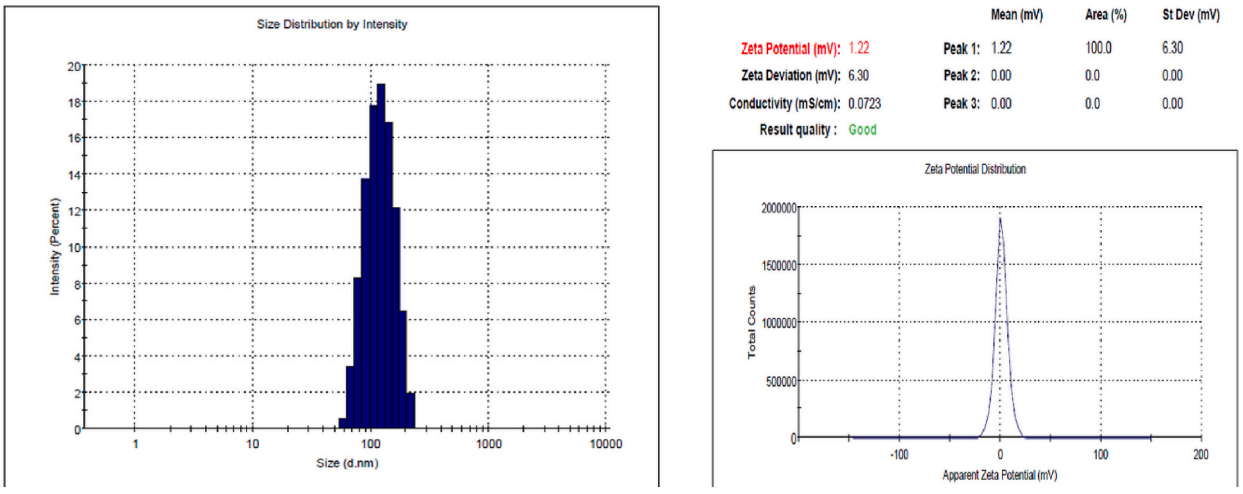

Fig. 5. DLS and Zeta potential analysis of green synthesized AgNPs. (For interpretation of the references to colour in this figure legend, the reader is referred to the Web version of this article.)

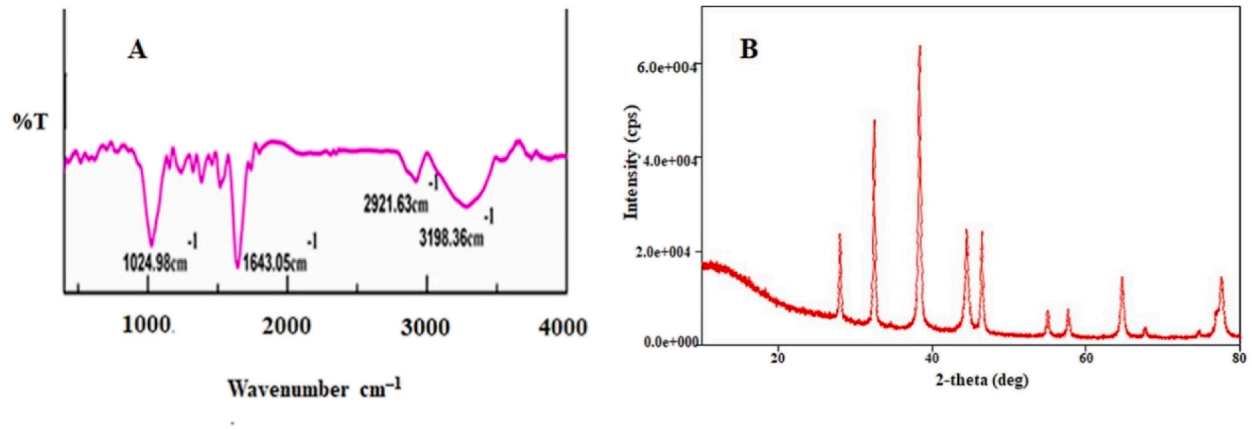

Fig. 6. (A) FT-IR spectra, (B) X-ray diffraction pattern of synthesized AgNPs.

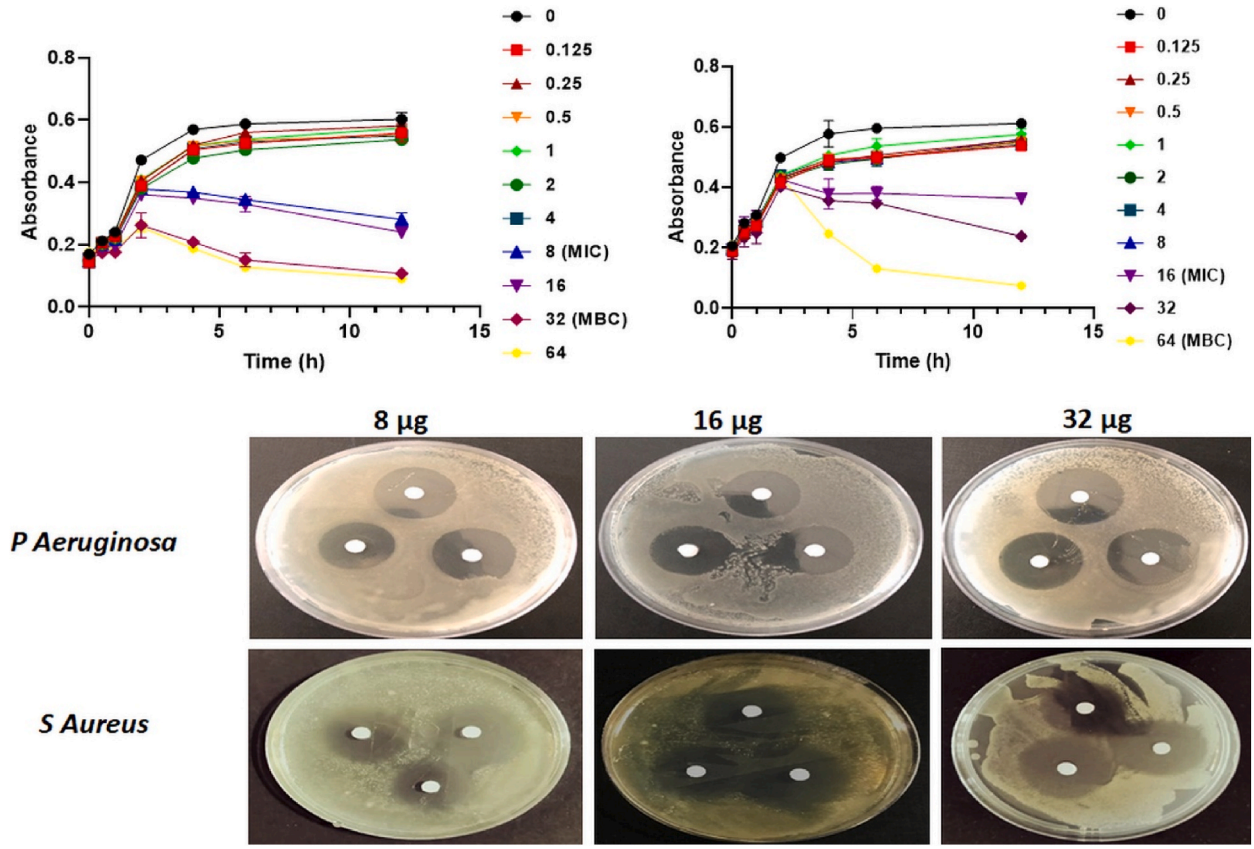

Fig. 7. (a) MIC and MBC of AgNPs against *P. aeruginosa* and *S. aureus* respectively, (b) Study of the zone of inhibition potency of green synthesized AgNPs. (For interpretation of the references to colour in this figure legend, the reader is referred to the Web version of this article.)

3.5. Evaluation of biological activity

3.5.1. Antimicrobial and antibiofilm study

Nowadays, many bacteria are gradually becoming resistant due to their biofilm formation [36]. These biofilms are difficult to eradicate and are the source of many persistent infections. Bacteria embedded in a biofilm can withstand high concentrations of bactericidal antibiotics while remaining fully susceptible to such antibiotics in vitro under planktonic conditions [37]. Therefore, viable antimicrobial therapy should target bacterial biofilms to break down the resistant mechanism of pathogenic bacteria.

3.5.1.1. Minimum inhibitory concentration (MIC) and minimum bactericidal concentration (MBC) determination. The potency of green synthesized AgNPs against both resistant gram-positive and gram-negative bacteria has been correlated with the destruction of bacterial membranes and drainage of intracellular material to cause bacterial death [11,21]. We found the MICs of green synthesized AgNPs to be 8 μg/mL and 16 μg/mL, respectively, against *P. aeruginosa* and *S. aureus* [Fig. 7 (a)]. Similar work has reported the minimum inhibitory concentration (MIC) of antibacterial AgNPs synthesized from *Pseudoduganella eburnea* MAHUQ-39 to be 6.25 μg/mL and 100 μg/mL for *P. aeruginosa* and *S. aureus* respectively [38]. Hence, our green synthesized AgNPs strongly inhibited the proliferation of both of the pathogens i.e., *P. aeruginosa* and *S. aureus*. Additionally, the AgNPs possessed MBC of 32 μg/mL and 65 μg/mL against these two bacterial species respectively. Therefore, these AgNPs acted as a potent inhibitor of the growth of both gram-positive and gram-negative bacteria at lower concentrations, and at higher concentrations, they ensured complete bacterial cell death.

3.5.1.2. Zone of inhibition study. Measurement of the zone of inhibition indicates bacterial susceptibility towards antimicrobial therapy over a surface and a greater zone assures the better efficacy of antimicrobial agents. The synthesized AgNPs displayed the dose-dependent zone of inhibition with 29 mm and 33 mm zone at a concentration 32 μg/mL against *P. aeruginosa* and *S. aureus*, respectively [Fig. 7 (b)]. These values indicate satisfactory antibacterial activity against both the microorganisms tested [25].

3.5.1.3. Antibiofilm activity. In the Live/Dead staining, green dye SYTO-9 penetrates both living and dead cells, whereas red PI stain penetrates only dead cells. The 3D images captured by confocal fluorescence microscope [Fig. 8] showed the bacterial films of *P. aeruginosa* and *S. aureus*, treated with the highest AgNPs concentration (32 μg/mL), have more red cells (PI labelled) than the cells treated with 8, 16 μg/mL of AgNPs. This indicated the deeper penetration of AgNPs into the biofilms at the higher dose. In comparison to PI-labelling, the 8 g/mL dose showed a greater population of SYTO-9 labelled live cells.

Both *P. aeruginosa* and *S. aureus* frequently are known to cause chronic, AMR infections due to their ability to form recalcitrant biofilms. This allows these organisms to resist bactericidal action of common antibacterial agents [39]. Our results indicated that Nishamalaki mediated AgNPs acquire remarkable concentration dependent potency in invading the complex microbial films of both of the bacteria tested, i.e., *P. aeruginosa* and *S. aureus*, to successfully eliminate them.

3.5.2. Anti-oxidant activity

The production of reactive oxygen species by pathogenic bacteria is a crucial factor in the biofilm formation, although the exact pathway and mechanism are still debatable. However, antimicrobial agents with good antioxidant effects can be a better option for the destruction of biofilms by ROS scavenging process [40,41]. The antioxidant potency of the Nishamalaki mediated AgNPs was studied by DPPH free radical scavenging method and the results showed high efficacy of AgNPs in comparison to the Nishamalaki churna extract. The calculated IC_{50} values of the Standard ascorbic acid, green synthesized silver nanoparticles and aqueous extract of Nishamalaki churna were respectively as 23.95 μg/mL, 28.93 μg/mL and 31.74 μg/mL. This confirmed that our AgNPs are capable of inducing a strong antioxidant effect to target resistant bacteria.

3.5.3. Anti-inflammatory activity

Protein denaturation, occurring during microbial infection, is one of the prime reasons behind inflammation. Microbes frequently activate the inflammatory enzymes or transcription factors by ROS production [42]. Consequently, it is anticipated that an antimicrobial drug with an associated anti-inflammatory action will be very successful in treating complex microbial infections. An antimicrobial agent with added anti-inflammatory, as well as antioxidant effects, can turn out to be a potent lead in the search for an effective antimicrobial agent.

In this research, the protective effect of synthesized AgNPs (5–100 μg/mL) against protein denaturation was studied in comparison to Nishamalaki churna extract as well as the standard reference drug Diclofenac sodium. The Nishamalaki mediated AgNPs showed concentration dependant inhibition of protein denaturation with IC_{50} of 21.76 μg/mL, thereby having great potential to act as an effective anti-inflammatory agent.

3.5.4. Cell viability study

MTT assay was done on HEK 293 cell lines to assess the safety of the synthesized AgNPs. The results showed 76 $\pm$ 2.96% and 59.20 $\pm$ 1.78% cell viability at 500 μg/mL dose for 24 h and 48 h, respectively. Selectivity index (SI) for antimicrobial agents can be estimated as the ratio of the toxic concentration of a sample against its effective bioactive concentration [43]. Generally, SI $\geq$ 10 is recommended acceptance criterion for a safe bioactive sample [44]. We found the MICs of our green synthesized AgNPs to be 8 μg/mL and 16 μg/mL, respectively, against *P. aeruginosa* and *S. aureus*. Our synthesized AgNps, having very high SI value, can therefore be considered safe for therapeutic applications.

4. Conclusion

In the present study, easy and one-step facile synthesis of silver nanoparticles was carried out using the aqueous extract of Nishamalaki churna. The phytochemical study of the Nishamalaki churna extract revealed a well manage phytoconstituent frame of the formulation with a notable quantity of phenols and flavonoids to be factors for successful synthesis, capping and stabilization of AgNPs. By the virtue of the anti-biofilm activity, these AgNPs demonstrated promising effects in the treatment of resistant bacterial infections.

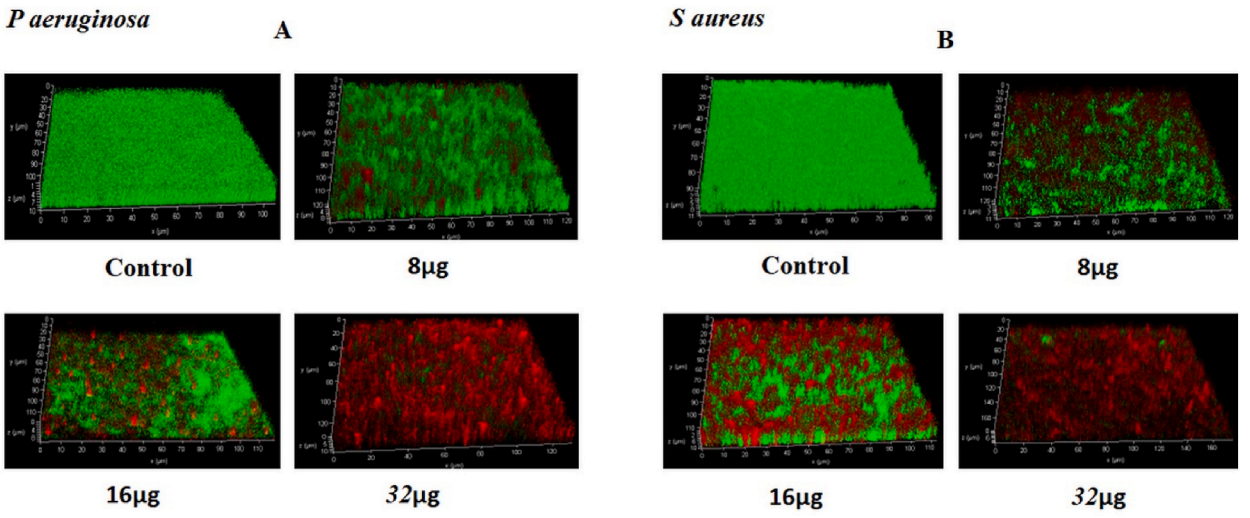

Fig. 8. Study of anti-biofilm activity of green synthesized AgNPs against (A) *P. aeruginosa* and (B) *S. aureus*. (For interpretation of the references to colour in this figure legend, the reader is referred to the Web version of this article.)

Additionally, these nanoparticles were endowed with antioxidant and anti-inflammatory activities, desirable by an ideal antibacterial agent. It would therefore be worthy to apply these synthesized AgNPs for treating localized skin infections as well for healing infected wounds. However, in vivo studies are necessary using different animal models for the confirmation of these biological activities of our synthesized AgNPs.

Funding

This work has been partially supported by All India Council for Technical Education [File No. 8-65/FDC/RPS (POLICY-l)/2019–20] sanctioned to Prof. Anindya Bose under Research Promotion Scheme (RPS) and DBT-BUILDER grant of Interdisciplinary Life Science Programme for Advance Research and Education (File No. BT/INF/22/SP45078/2022) sanctioned to Siksha O Anusandhan, Bhubaneswar.

Author contribution statement

Bhavna Ghosh: performed the experiments; analyzed and interpreted the data; wrote the paper.
Anindya Bose: conceived and designed the experiments; analyzed and interpreted the data; wrote the paper.
Ankita Parmanik: performed the experiments; wrote the paper.
Sanjay Ch: performed the experiments; analyzed and interpreted the data; Milan Paul: performed the experiments; analyzed and interpreted the data; Swati Biswas: analyzed and interpreted the data; Goutam Rath: analyzed and interpreted the data; Debapriya Bhattacharya: analyzed and interpreted the data.

Data availability statement

Data included in article/supp. material/referenced in article.

Declaration of competing interest

The authors declare that they have no known competing financial interests or personal relationships that could have appeared to influence the work reported in this paper.

References

[1] T. Thompson, The staggering death toll of drug-resistant bacteria, Eupb ahead of print (2022), Nature (2022), 10. 1038/d41586-022-00228-x.
[2] A.L. Spoering, K.I.M. Lewis, Biofilms and planktonic cells of Pseudomonas aeruginosa have similar resistance to killing by antimicrobials, JOB 183 (23) (2001) 6746–6751, https://doi.org/10.1128/JB.183.23.6746-6751.2001.
[3] R. Sharma, A. Bhatt, M. Thakur, Physicochemical characterization and antibacterial activity of Rajata Bhasma and silver nanoparticle, Ayu 37 (1) (2016) 71–75, https://doi.org/10.4103/ayu.AYU_167_15.
[4] T. Jaswal, J. Gupta, A review on the toxicity of silver nanoparticles on human health, Materials (2021), https://doi.org/10.1016/j.matpr.2021.04.266.
[5] S.M. Ghaseminezhad, S. Hamedi, S.A. Shojaosadati, Green synthesis of silver nanoparticles by a novel method: comparative study of their properties, Carbohydr. Polym. 89 (2) (2012) 467–472, https://doi.org/10.1016/j.carbpol.2012.03.030.

[6] G. Venkateshwarlu, N.C.H. Venkata, T.R. Shantha, K.R. Kishore, R.M. Prathapa, H.L. Raghavendra, A comparative physicochemical and pharmacognostical evaluation of nishamalaki-an ayurvedic antidiabetic formulation, Sci. Technol. Arts Res. J. 2 (3) (2013) 69–78.

[7] F.M. Abdel Bar, M.M. Abu Habib, F.A. Badria, A new hexagalloyl compound from Emblica officinalis Gaertn, Antioxid. Cytotox. Silver Ion Red. Activi.CP 75 (12) (2021) 6509–6518, https://doi.org/10.1007/s11696-021-01810-9.

[8] F.K. Alsammarraie, W. Wang, P. Zhou, A. Mustapha, M. Lin, Green synthesis of silver nanoparticles using turmeric extracts and investigation of their antibacterial activities, Colloids Surf., B 171 (2018) 398–405, https://doi.org/10.1016/j.colsurfb.2018.07.059.

[9] D.A. Selvan, D. Mahendiran, R.S. Kumar, A.K. Rahiman, Garlic, green tea and turmeric extracts-mediated green synthesis of silver nanoparticles: phytochemical, antioxidant and in vitro cytotoxicity studies, J. Photochem. Photobiol. B Biol. 180 (2018) 243–252, https://doi.org/10.1016/j.jphotobiol.2018.02.014.

[10] M.N. Nadagouda, N. Iyanna, J. Lalley, C. Han, D.D. Dionysiou, R.S. Varma, Synthesis of silver and gold nanoparticles using antioxidants from blackberry, blueberry, pomegranate, and turmeric extracts, ACS Sustain. Chem. Eng. 2 (7) (2014) 1717–1723, https://doi.org/10.1021/sc500237k.

[11] P.S. Ramesh, T. Kokila, D. Geetha, Plant mediated green synthesis and antibacterial activity of silver nanoparticles using Emblica officinalis fruit extract, Spectrochim. Acta Mol. Biomol. Spectrosc. 142 (2015) 339–343, https://doi.org/10.1016/j.saa.2015.01.062.

[12] F.S. Rosarin, V. Arulmozhi, S. Nagarajan, S. Mirunalini, Antiproliferative effect of silver nanoparticles synthesized using amla on Hep2 cell line, Asian Pac. J. Tropical Med. 6 (1) (2013) 1–10, https://doi.org/10.1016/S1995-7645(12)60193-X.

[13] J. Singh, T. Singh, M. Rawat, Green synthesis of silver nanoparticles via various plant extracts for anti-cancer applications, Glob. J. Nanomed. 2 (3) (2017) 1–4, https://doi.org/10.19080/GJN.2017.02.555590.

[14] S. Ranjani, K. Tamanna, S. Hemalatha, Triphala green nano colloids: synthesis, characterization and screening biomarkers, Appl. Nanosci. 10 (4) (2020) 1269–1279, https://doi.org/10.1007/s13204-019-01208-w.

[15] A. Parmanik, A. Bose, B. Ghosh, M. Paul, A. Itoo, S. Biswas, M. Arakha, Development of triphala churna extract mediated iron oxide nanoparticles as novel treatment strategy for triple negative breast cancer, J. Drug Deliv. Sci. Technol. 76 (2022), 103735, https://doi.org/10.1016/j.jddst.2022.103735.

[16] S. Mukhi, A. Bose, A. Ray, P.K. Swain, Analytical standards of Amrtadi Churna: a classical ayurvedic formulation, Indian J. Pharmaceut. Sci. 79 (2) (2017) 227–240, https://doi.org/10.4172/pharmaceutical-sciences.1000221.

[17] R. Arutselvi, T. Balasaravanan, P. Ponmurugan, N.M. Saranji, P. Suresh, Phytochemical screening and comparative study of anti microbial activity of leaves and rhizomes of turmeric varieties, Asian J. Plant Sci. Res. 2 (2) (2012) 212–219.

[18] J.B. Krajewska, O. Długosz, M. Sałaga, M. Banach, J. Fichna, Silver nanoparticles based on blackcurrant extract show potent anti-inflammatory effect in vitro and in DSS-induced colitis in mice, Int. J. Pharm. 585 (2020), 119549, https://doi.org/10.1016/j.ijpharm.2020.119549.

[19] A.O. Akintola, B.D. Kehinde, P.B. Ayoola, A.G. Adewoyin, O.T. Adedosu, J.F. Ajayi, S.B. Ogunsona, Antioxidant properties of silver nanoparticles biosynthesized from methanolic leaf extract of Blighia sapida, IOP Conf. Ser. Mater. Sci. Eng. 805 (2020), 012004, https://doi.org/10.1088/1757-899X/805/1/012004.

[20] L.K. Ruddaraju, P.N. Pallela, S.V. Pammi, V.S. Padavala, V.R. Kolapalli, Synergetic antibacterial and anticarcinogenic effects of Annona squamosa leaf extract mediated silver nano particles, Mater. Sci. Semicond. Process. 100 (2019) 301–309, https://doi.org/10.1016/j.mssp.2019.05.007.

[21] K.M. Kumar, M. Sinha, B.K. Mandal, A.R. Ghosh, K.S. Kumar, P.S. Reddy, Green synthesis of silver nanoparticles using Terminalia chebula extract at room temperature and their antimicrobial studies, Spectrochim. Acta Mol. Biomol. Spectrosc. 91 (2012) 228–233, https://doi.org/10.1016/j.saa.2012.02.001.

[22] A.K. Mittal, A. Kaler, U.C. Banerjee, Free radical scavenging and antioxidant activity of silver nanoparticles synthesized from flower extract of Rhododendron dauricum, Nano Biomed. Eng. 4 (3) (2012) 118–124, https://doi.org/10.5101/nbe.v4i3.p118-124.

[23] S.N. Kharat, V.D. Mendhulkar, Synthesis, characterization and studies on antioxidant activity of silver nanoparticles using Elephantopus scaber leaf extract, Mater. Sci. Eng., C 62 (2016) 719–724, https://doi.org/10.1016/j.msec.2016.02.024.

[24] S. Rajput, D. Kumar, V. Agrawal, Green synthesis of silver nanoparticles using Indian Belladonna extract and their potential antioxidant, anti-inflammatory, anticancer and larvicidal activities, Plant Cell Rep. 39 (2020) 921–939, https://doi.org/10.1007/s00299-020-02539-7.

[25] P. Das, K. Ghosal, N.K. Jana, A. Mukherjee, P. Basak, Green synthesis and characterization of silver nanoparticles using belladonna mother tincture and its efficacy as a potential antibacterial and anti-inflammatory agent, Mater. Chem. Phys. 228 (2019) 310–317, https://doi.org/10.1016/j.matchemphys.2019.02.064.

[26] H.H. Lara, E.N. Garza-Treviño, L. Ixtepan-Turrent, D.K. Singh, Silver nanoparticles are broad-spectrum bactericidal and virucidal compounds, J. Nanobiotechnol. 9 (1) (2011) 1–8, https://doi.org/10.1186/1477-3155-9-30.

[27] H.H. Lara, N.V. Ayala-Núnez, L.D.C. Ixtepan Turrent, C. Rodríguez Padilla, Bactericidal effect of silver nanoparticles against multidrug-resistant bacteria, 2010, World J. Microbiol. Biotechnol. 26 (4) (2010) 615–621, https://doi.org/10.1007/s11274-009-0211-3.

[28] G. Franci, A. Falanga, S. Galdiero, L. Palomba, M. Rai, G. Morelli, M. Galdiero, Silver nanoparticles as potential antibacterial agents, Molecules 20 (5) (2015) 8856–8874, https://doi.org/10.3390/molecules20058856.

[29] S.A. Ahmad, S.S. Das, A. Khatoon, M.T. Ansari, M. Afzal, M.S. Hasnain, A.K. Nayak, Bactericidal activity of silver nanoparticles: a mechanistic review, Mater. Sci. Technol. 3 (2020) 756–769, https://doi.org/10.1016/j.mset.2020.09.002.

[30] R. Manikandan, M. Beulaja, R. Thiagarajan, S. Palanisamy, G. Goutham, A. Koodalingam, N.M. Prabhu, E. Kannapiran, M.J. Basu, C. Arulvasu, M. Arumugam, Biosynthesis of silver nanoparticles using aqueous extract of Phyllanthus acidus L. fruits and characterization of its anti-inflammatory effect against H2O2 exposed rat peritoneal macrophages, Process Biochem. 55 (2017) 172–181, https://doi.org/10.1016/j.procbio.2017.01.023.

[31] M.M. Masum, M.M. Siddiqa, K.A. Ali, Y. Zhang, Y. Abdallah, E. Ibrahim, W. Qiu, C. Yan, B. Li, Biogenic synthesis of silver nanoparticles using Phyllanthus emblica fruit extract and its inhibitory action against the pathogen Acidovorax oryzae strain RS-2 of rice bacterial brown stripe, Front. Microbiol. 10 (2019) 820, https://doi.org/10.3389/fmicb.2019.00820.

[32] A. Zielińska, E. Skwarek, A. Zaleska, M. Gazda, J. Hupka, Preparation of silver nanoparticles with controlled particle size, Procedia Chem. 1 (2) (2009) 1560–1566, https://doi.org/10.1016/j.proche.2009.11.004.

[33] B. Kumar, K. Smita, L. Cumbal, A. Debut, Green synthesis of silver nanoparticles using Andean blackberry fruit extract, Saudi J. Biol. Sci. 24 (1) (2017) 45–50, https://doi.org/10.1016/j.sjbs.2015.09.006.

[34] S. Priyadarshini, S. Sulava, R. Bhol, S. Jena, Green synthesis of silver nanoparticles using Azadirachta indica and Ocimum sanctum leaf extract, Curr. Sci. 117 (2019) 1300–1307.

[35] P.B. Kedi, F.E. Meva, L. Kotsedi, E.L. Nguemfo, C.B. Zangueu, A.A. Ntoumba, H.E. Mohamed, A.B. Dongmo, M. Maaza, Eco-friendly synthesis, characterization, in vitro and in vivo anti-inflammatory activity of silver nanoparticle-mediated Selaginella myosurus aqueous extract, Int. J. Nanomed. 13 (2018) 8537–8548, https://doi.org/10.2147/IJN.S174530.

[36] A. Algburi, N. Comito, D. Kashtanov, L.M. Dicks, M.L. Chikindas, Control of biofilm formation: antibiotics and beyond, Appl. Environ. Microbiol. 83 (3) (2017), e02508-e02516, https://doi.org/10.1128/AEM.02508-16.

[37] J.N. Anderl, M.J. Franklin, P.S. Stewart, Role of antibiotic penetration limitation in Klebsiella pneumoniae biofilm resistance to ampicillin and ciprofloxacin, Antimicrob. Agents Chemother. 44 (7) (2000) 1818–1824, https://doi.org/10.1128/AAC.44.7.1818-1824.2000.

[38] M.A. Huq, Green synthesis of silver nanoparticles using *Pseudoduganella eburnea* MAHUQ-39 and their antimicrobial mechanisms investigation against drug resistant human pathogens, Int. J. Mol. Sci. 21 (4) (2020) 1510, https://doi.org/10.3390/ijms21041510.

[39] Giulia Orazi, Kathryn L. Ruoff, George A. O'Toole, Pseudomonas aeruginosa increases the sensitivity of biofilm-grown Staphylococcus aureus to membrane-targeting antiseptics and antibiotics, mBio 10 (4) (2019), e01501-e01519, https://doi.org/10.1128/mBio.01501-19.

[40] K.S. Ong, C.I. Mawang, D. Daniel-Jambun, Y.Y. Lim, S.M. Lee, Current anti-biofilm strategies and potential of antioxidants in biofilm control, Expert Rev. Anti Infect. Ther. 16 (11) (2018) 855–864, https://doi.org/10.1080/14787210.2018.1535898.

[41] S. Jagani, R. Chelikani, D.S. Kim, Effects of phenol and natural phenolic compounds on biofilm formation by Pseudomonas aeruginosa, Biofouling 25 (4) (2009) 321–324, https://doi.org/10.1080/08927010802660854.

[42] H. Agarwal, A. Nakara, V.K. Shanmugam, Anti-inflammatory mechanism of various metal and metal oxide nanoparticles synthesized using plant extracts: a review, Biomed. Pharmacother. 109 (2019) 2561–2572, https://doi.org/10.1016/j.biopha.2018.11.116.
[43] J.C. Pritchett, L. Naesens, J. Montoya, L. Flamand, I. Lautenschlager, G.R. Krueger, D.V. Ablashi, Treating HHV-6 infections: the laboratory efficacy and clinical use of ati-HHV-6 infections, Clin. Microbiol. Rev. 28 (2) (2015) 313–335, https://doi.org/10.1128/CMR.00122-14.
[44] M.D. Awouafack, L.J. McGaw, S. Gottfried, R. Mbouangouere, P. Tane, M. Spiteller, J.N. Eloff, Antimicrobial activity and cytotoxicity of the ethanol extract, fractions and eight compounds isolated from Eriosema robustum (Fabaceae), BMC Compl. Alternative Med. 13 (2013) 289, https://doi.org/10.1186/1472-6882-13-289.